Effect of Bismuth Doping on Noise Figure of Er-Doped Silica Fiber

Weizhu Ji, Jianxiang Wen, Yanhua Dong, Junnan Zhang, Xiuxiu Chen, Yan Chen, Zexin Zheng, and Tingyun Wang, *Member, IEEE*

***Abstract*—We investigate the spectral and amplification characteristics of Bi/Er co-doped fiber (BEDF) and Er-doped fiber (EDF), prepared by atomic layer deposition (ALD). BEDF features a noise figure (NF) below 5.2 dB, the bandwidth with NF less than 4 dB is approximately 23 nm (1560–1583 nm), and that with a gain exceeding 25 dB is approximately 42 nm (1525–1567 nm). The quantum conversion efficiency (QCE) of BEDF at 1550 nm is 72.1% at a pump power of 300 mW. The saturated output power of BEDF at 1550 nm is 21.4 dBm. Raman spectra indicate that the maximum phonon energy of BEDF is lower than that of EDF. The fluorescence lifetime of the BEDF is 11.64 ms, which is longer than that of the EDF. These results show that co-doping with Bi ions could increase the fluorescence lifetime of Er^{3+}, reduce the NF, and improve the QCE and saturated output power. Therefore, this type of BEDF is a promising gain medium for optical amplifiers and lasers.**

***Index Terms*—Bi/Er co-doped fiber, noise figure, conversion efficiency, fluorescence lifetime, optical communication.**

I. Introduction

THE capacity of optical fiber communication is expanding with the advent of 5G+/6G communication, intelligent world, and Internet of Everything [1]. Currently, Er-doped fiber amplifiers (EDFAs) are widely utilized for optical amplification because of their ability to fully exploit the low-loss communication window of silica fibers [2]. However, its bandwidth is limited due to the 4f-4f orbital limiting effect of Er^{3+} [3]. Moreover, EDFA can produce amplified spontaneous emission (ASE), which is the main noise source of the amplifier and reduces the signal-to-noise ratio of the transmission. It is hardly eliminated when the frequency of the ASE is the same as that of the signal, which can reduce the sensitivity of the receiver and lead to an increase in the bit error rate because it is converted into electrical noise in the optical receiver [4]. Therefore, there is a great demand for active media with a lower noise figure (NF) and higher gain.

It is well known that Bi ions have an unshielded outer electron shell, as opposed to rare-earth elements. Bi ions can combine with different elements to multiply bismuth active centers (BACs), such as aluminum (BAC-Al), phosphorus (BAC-P), silica (BAC-Si), and germanium (BAC-Ge) [5], [6]. Considering that the spectral range of Bi is adjacent to that of Er, Bi/Er co-doped fibers (BEDF) could yield ultrawideband fluorescence spectra [7], [8]. Therefore, BEDFs have attracted the interest of researchers working in a wide range of research areas. Co-doping with Bi ions could enhance the emission intensity by suppressing the up-conversion luminescence of Er^{3+} and inhibiting the concentration quenching effect of Er^{3+} [9]. A recent report has shown that energy transfer from BAC-Al to Er^{3+} under 830 nm pumping could increase the on-off gain and fluorescence lifetime of Er^{3+} at 1536 nm [10]. Furthermore, many studies on the amplification characteristics of BEDF have been conducted. An on-off gain of over 2.4 dB/m was observed over the spectral range of 1300–1600 nm and the maximum on-off gain were 5.87 dB. However, the gain intensity remained weak [11], [12]. A Bi/Er co-doped germanosilicate fiber was reported with a 15 dB small-signal gain band covering 260 nm from 1515 to 1775 nm, but its NF was higher at 7–10 dB [13]. A newly fabricated hafnia-bismuth erbium co-doped fiber was reported with a flat gain of 12.1 dB along the wavelength region of 80 nm from 1525 to 1605 nm with an NF of up to 11.8 dB [14]. Qiu et al. proposed a relatively novel method to reduce NF by introducing the central depressed refractive index and narrowing the erbium doping region [15]. In conclusion, their gain intensity remains low, NF remains high, and research on the influence of Bi ions on the noise characteristics of Er^{3+} remains rare. Therefore, it is crucial to investigate the effect of Bi doping on the noise characteristics of the Er^{3+} ions.

In this study, two types of fiber samples, namely BEDF and Er-doped fiber (EDF), were fabricated by modified chemical vapor deposition (MCVD) along with atomic layer deposition (ALD). The optical properties of BEDF were investigated, including the absorption spectra, Raman spectra, fluorescence lifetime, and unsaturated loss (UL). In addition, the amplification characteristics of BEDF under different conditions were systematically studied.

Manuscript received 19 October 2022; revised 4 February 2023; accepted 15 February 2023. Date of publication 20 February 2023; date of current version 3 March 2023. This work was supported in part by the National Key Research and Development Projects under Grant 2020YFB1805800, in part by the National Natural Science Foundation of China under Grants 62027818, 61975113, and 61935002, and in part by the Shanghai Professional Technical Public Service Platform of Advanced Optical Waveguide Intelligent Manufacturing and Testing under Grant 19DZ2294000. *(Corresponding author: Tingyun Wang.)*

The authors are with the Key Laboratory of Specialty Fiber Optics and Optical Access Networks, Joint International Research Laboratory of Specialty Fiber Optics and Advanced Communication, Shanghai Institute for Advanced Communication and Data Science, Shanghai University, Shanghai 200444, China (e-mail: 3186175630@qq.com; wenjx@shu.edu.cn; dongyanhua@shu.edu.cn; 961977559@qq.com; 2426016374@qq.com; 2628295252@qq.com; 1455823314@qq.com; tywang@shu.edu.cn).

Digital Object Identifier 10.1109/JPHOT.2023.3246538

TABLE I
THE ELEMENT COMPOSITIONS OF FIBER SAMPLES

Element	EDF (at%)	BEDF1 (at%)	BEDF2 (at%)
Bi	/	0.013	0.021
Er	0.022	0.022	0.024
P	0.819	0.805	0.835
Al	0.469	0.471	0.504
Ge	1.011	1.105	1.102
Si	32.842	32.543	32.463
O	64.837	65.041	65.051

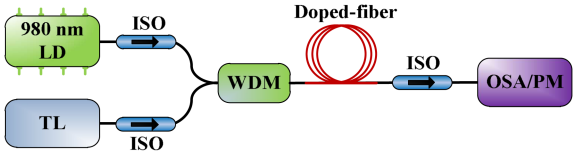

Fig. 1. Optical amplification measurement system of the doped-fiber. TL: Tunable Laser; 980 nm LD: 980 nm laser diode; WDM: wavelength division multiplexer; Doped-fiber: EDF or BEDF; ISO: isolator; OSA: optical spectrum analyzer; PM: power meter.

II. EXPERIMENTAL SETUP

For this study, EDF, BEDF1 and BEDF2 were prepared using ALD (TFS-200, Beneq Inc., Finland) combined with the MCVD technique [16], [17]. The core compositions of EDF, BEDF1 and BEDF2 were measured using an electron probe microanalyzer (Shimadzu EPMA-8050G, Japan). The element compositions of EDF, BEDF1 and BEDF2 are summarized in Table I. The concentration of Bi in BEDFs is optimized to avoid the high background loss caused by high Bi doping concentration. Small amounts of Al, P, and Ge were co-doped with the optical fiber to prevent ion quenching, suppress the photodarkening effect, and inhibit the decrease in the refractive index at the core center, respectively [18], [19]. The cross sections of the three samples were measured using an optical microscope (Olympus Bx43, Japan), and the refractive index difference (RID) of the fibers was analyzed using an optical fiber refractive index analyzer (S14, Photon Kinetics Inc., USA). The core and cladding diameters of EDF, BEDF1 and BEDF2 are 8.16/125.42, 8.21/125.41, and 8.24/125.51 μm, respectively. The RID of EDF, BEDF1 and BEDF2 between the fiber core and cladding were approximately 0.0054, 0.0054, and 0.0057, respectively.

A broadband white light source (AQ-4305, Yokogawa, Japan) was used to measure the optical absorption spectrum using the traditional cutback method. The UL were also measured with 976 and 1550 nm laser diodes. Moreover, the Raman spectra in the range of 200–1500 cm^{-1} were recorded using a LabRam HR Evolution Raman spectrometer (LabRam HR800, Horiba Jobin Yvon, France) with a laser wavelength of 633 nm. The excitation and emission spectra and fluorescence lifetime of the doped fibers were measured using a fluorescence spectrometer (FLS 980, Edinburgh Instruments Inc., England), equipped with a red-sensitive single-photon counting photomultiplier (Hamamatsu R928P) and placed in a Peltier air-cooled enclosure. All the aforementioned-tests were conducted at room temperature.

Furthermore, a conventional forward-pumping scheme was used to achieve better noise characteristics, as shown in Fig. 1.

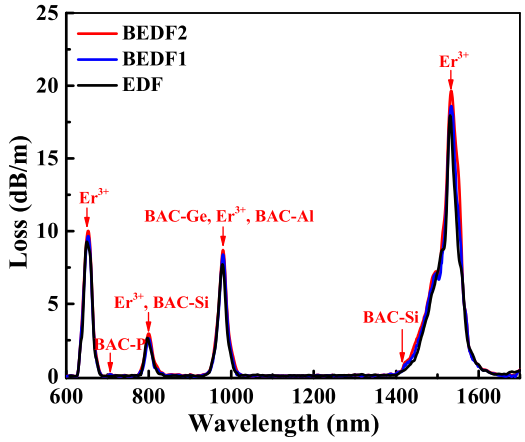

Fig. 2. The absorption spectra of EDF, BEDF1 and BEDF2.

The lengths of BEDF2 and EDF used in this study are optimal for 10 and 8 m, respectively. Short fibers can avoid the increase in NF caused by Rayleigh scattering [20]. In this measurement system, a tunable laser (Santec TSL-710, Japan) operating in the spectral range of 1480–1640 nm was used as the signal source. An optical spectrum analyzer (OSA, Yokogawa AQ6370D, Japan) and a power meter (PM) were used to detect the amplified signal light. The OSA is used not only for peak-to-peak gain measurements but also for calculating the noise power at the signal wavelength using the interpolation method. Furthermore, the noise power was calibrated using a PM to ensure the test accuracy. The source subtraction technique described in [4], [21] and (1) were used to calculate NF.

$$NF = 10\log\left(\frac{P_{ase}}{GhvB_0} + \frac{1}{G} - \frac{P_{sse}}{hvB_0}\right) \tag{1}$$

where P_{ase} and P_{sse} are the output amplified spontaneous emission power and input source noise power at the signal wavelength, respectively; G denotes the signal gain; h is the Planck constant; v is the photon frequency; and B_0 denotes the efficient noise bandwidth at the signal wavelength.

The optical absorption spectra of three samples are shown in Fig. 2. The background losses of EDF, BEDF1 and BEDF2 at 1200 nm are 0.03, 0.03 and 0.02 dB/m, respectively. There are four distinct absorption bands of Er^{3+} in the BEDF samples at 654, 799, 980, and 1534 nm, attributed to $^4I_{15/2}\rightarrow{}^4F_{9/2}$, $^4I_{15/2}\rightarrow{}^4I_{9/2}$, $^4I_{15/2}\rightarrow{}^4I_{11/2}$, and $^4I_{15/2}\rightarrow{}^4I_{13/2}$ electronic transitions with corresponding absorption coefficients of 10.0, 3.0, 8.7 and 19.7 dB/m, respectively. The absorption intensity of BACs is low because of the low concentration Bi in BEDF2. BAC-P presents an absorption band at 700 nm; BAC-Si band mainly involved absorption bands around 812 and 1422 nm; BAC-Ge showed an absorption band at 950 nm; and BAC-Al exhibited absorption bands at 1000 nm [22]. The absorption coefficients of EDF at 650, 797, 977, and 1530 nm are 9.2, 2.7, 7.7, 18.2 dB/m, respectively. Compared with the absorption coefficients of EDF, due to the partial overlap of BACs and Er^{3+}, the absorption peak intensities of BEDF2 are enhanced, and the bandwidth is widened, and that of BEDF1 have little change due to the low Bi concentration [23].

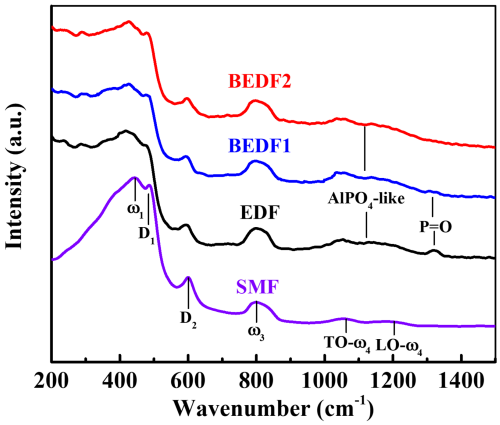

Fig. 3. Raman spectra of SMF, EDF, BEDF1 and BEDF2.

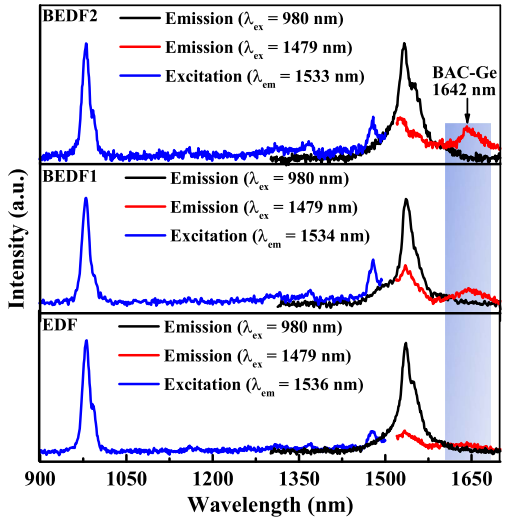

Fig. 4. Excitation and emission spectra of EDF, BEDF1 and BEDF2.

III. Results and Discussion

A. Raman Spectra

The Raman spectra of SMF (SMF-28, Corning Inc., America), EDF, and BEDFs in the range of 200–1500 cm^{-1} were measured to further analyze the changes in the microstructure of the silica optical fibers, as shown in Fig. 3. Six sharp peaks can be observed in the Raman spectrum of SMF, with a strong band peak at 440 cm^{-1} and five weak band peaks at 490, 606, 800, 1060, and 1200 cm^{-1}. The peaks at $D_1 = 490$ and $D_2 = 606$ cm^{-1} correspond to the symmetrical stretching vibrations of the planar four-fold and planar three-fold rings, respectively [24]. The peak at $\omega_1 = 440$ cm^{-1} results from the Si-O-Si symmetrical stretching vibration. On the other hand, the peak at $\omega_3 = 800$ cm^{-1} is attributed to the Si-O-Si bending vibration [25]. The 1060 and 1200 cm^{-1} bands are ascribed to transverse optical (TO) and longitudinal optical (LO) asymmetric stretching (TO-ω_4 and LO-ω_4) vibrations of the Si-O-Si bonds, respectively [26], [27]. All these peaks observed for SMF are also observed for EDF and BEDFs. However, compared with the Raman spectra of SMF, a wide band of 1000–1250 cm^{-1} can be observed for EDF and BEDFs. The wide band peak at 1145 cm^{-1} often corresponds to $AlPO_4$-like units, which provide the maximum photon energy for BEDF2 [28]. In addition, a narrow and sharp peak with a value of 1321 cm^{-1} can be observed for EDF, which is attributed to the stretching vibration of the P=O bond in the $P^{(3)}$ unit in the structural model O=P-$O_{3/2}$ [29], [30], [31]. This peak provides the maximum photon energy for EDF, which is not detected in the Raman spectrum of BEDF2 although the concentrations of phosphorus in EDF and BEDF2 samples are almost identical. And the Raman spectra of BEDF1 is similar to that of EDF except the peak at 1321 cm^{-1} is slightly weaker. Since the P=O bonds in silica are formed due to excess phosphorus, it is possible for Bi to bind with the excess P in some special form, thus hindering the formation of P=O bonds and reducing the maximum phonon energy of BEDF [32], [33].

B. Excitation and Emission Spectra

The excitation and emission spectra are presented in Fig. 4. The experimental results show two excitation peaks at 980 and 1479 nm in the excitation spectrum. The EDF, BEDF1 and BEDF2 samples are excited at 980 nm, and their emission peaks are at 1536, 1534 and 1533 nm, respectively, corresponding to the electron transition of Er^{3+} ions from $^4I_{11/2}$ to $^4I_{15/2}$. However, when the excitation wavelength is 1479 nm, the emission spectrum of BEDF1 and BEDF2 is slightly different from that of EDF, except for the electron transition of Er^{3+} ions from $^4I_{13/2}$ to $^4I_{15/2}$. The intensity of BEDF2 at 1642 nm is significantly higher than that of EDF. A new active center exists between Bi and Ge (BAC-Ge), resulting in an enhancement of the U-band emission intensity. The intensity of BAC-Ge at 1642 nm increases as the concentration of Bi doping increase. And the excitation and emission spectra of BEDF1 are similar to that of EDF. These phenomena indicate that BEDF can emit multiple luminescent centers with a wavelength excitation source, which is beneficial for widening the gain bandwidth and broadband luminescence. And it was found that the characteristics of BEDF1 with lower concentration Bi doping changed less through absorption spectra, Raman spectra, and excitation and emission spectra, therefore then we compared the characteristics of EDF and BEDF2 with a higher concentration Bi doping.

C. Fluorescence Decay Curve

The fluorescence decay curve of EDF and BEDF2 at the $^4I_{13/2}$ level was obtained after excitation at 980 nm, as shown in Fig. 5(a). The measured fluorescence lifetimes of EDF and BEDF2 are 9.77 and 11.64 ms, respectively. The fluorescence lifetime of Er^{3+} in the BEDF2 is longer than that of EDF, which is an increase of 1.87 ms.

The fluorescence lifetime is related to phonon energy of the fiber and energy transfer between different ions. If we try to neglect the energy transfer processes, the relationship between the measured fluorescence lifetime (τ_m), radiative lifetime (τ_r), and non-radiative lifetime (τ_{nr}) is given by (2) [34]:

$$\frac{1}{\tau_m} = \frac{1}{\tau_r} + \frac{1}{\tau_{nr}} \tag{2}$$

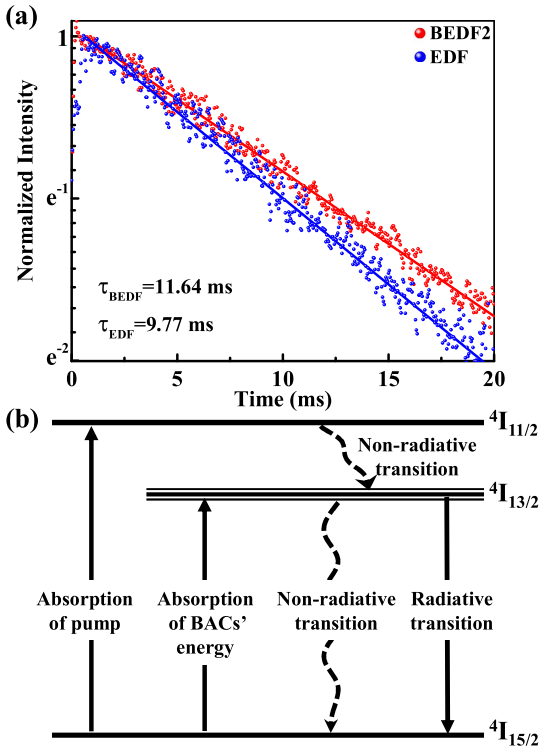

Fig. 5. Fluorescence lifetime of BEDF2 and EDF (a), and Er^{3+} particles state between energy levels (b).

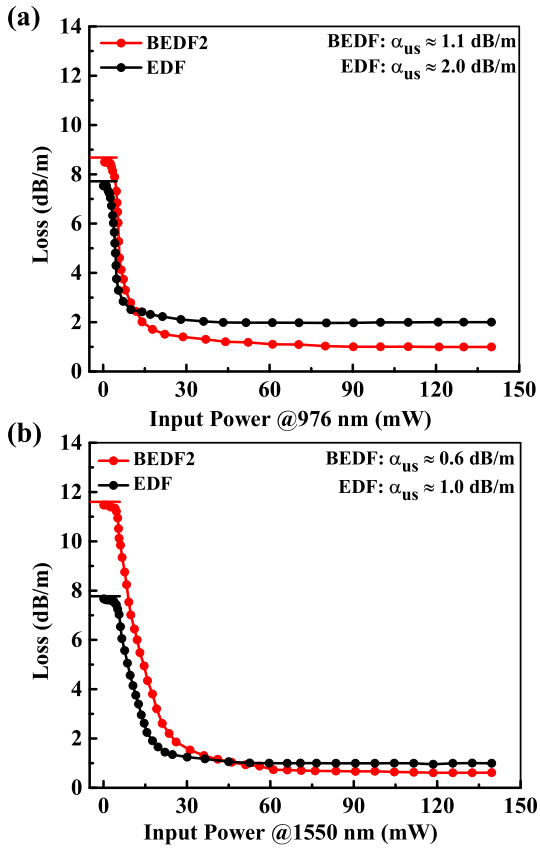

Fig. 6. Signal absorption of BEDF2 and EDF at 976 nm (a) and 1550 nm (b) vs input power.

The non-radiative lifetime depends largely on the phonon energy. Multi-phonon resonance could lead to the non-radiative relaxation of Er^{3+} particles from the upper level to the lower level, resulting in an energy loss and a reduction in the number of particles at upper level. The larger the phonon energy, the stronger is the multi-phonon relaxation process, resulting in an increase in the probability of non-radiative transition and a decrease in the non-radiative lifetime. According to the Raman spectra, the maximum phonon energy of BEDF2 is lower than that of EDF. The reduction in the maximum phonon energy can weaken the multi-phonon relaxation process, reduce the probability of non-radiative transition, and enhance τ_{nr}. In addition, it may present an energy transfer from BACs to Er^{3+} to enhance τ_r of Er^{3+}. These combined effects could lead to an increase in τ_m.

Fig. 5(b) illustrates the state of Er^{3+} particles between energy levels. After absorbing the 980 nm excitation light, the electrons of Er^{3+} ions migrate from the ground state, $^4I_{15/2}$ to the excited state, $^4I_{11/2}$. Then, the electrons in the excited state $^4I_{11/2}$ undergo a non-radiative transition to the metastable level, $^4I_{13/2}$ through phonon resonance. In addition, the electrons of Er^{3+} particles at the $^4I_{13/2}$ level undergo radiative and non-radiative transitions to reach the $^4I_{15/2}$ level. The non-radiative transition rate from the metastable level, $^4I_{13/2}$ to the ground level, $^4I_{15/2}$ decreases owing to the decrease in phonon energy. And the electrons of Er^{3+} particles at the $^4I_{15/2}$ level absorb the energy from BACs at the excited state, thus exciting to the $^4I_{13/2}$ level. As a result, this would lead to an increase in the electron numbers of Er^{3+} particles at the $^4I_{13/2}$ level, releasing more photons through radiative transition, thereby enhancing the fluorescence lifetime [35], [36].

D. Unsaturated Loss Characteristics

The UL at 976 nm was measured to understand the actual pump utilization efficiency at the absorption wavelength, while the UL at 1550 nm was measured to determine the effect of UL on the luminous efficiency at the emission wavelength. The UL levels at 976 nm absorption wavelength for BEDF2 and EDF are shown in Fig. 6(a), which are measured to be approximately 1.1 and 2.0 dB/m, respectively. The ratio of small-signal absorption (SSA) to UL at 976 nm in BEDF2 sample is approximately 8.7, which is higher than that of EDF (approximately 3.9). The pump utilization efficiency of BEDF2 at 976 nm is higher. Besides, the level of UL at 1550 nm emission wavelength of BEDF2 and EDF are presented in Fig. 6(b), which are approximately 0.6 and 1.0 dB/m, respectively. The SSA to UL ratios at 1550 nm are approximately 19.9 and 7.6, respectively. Compared with the UL level at the emission wavelength in EDF sample, the effect of UL on the luminous efficiency of BEDF2 is weaker. The UL level depends moderately on the wavelength, while UL at shorter wavelengths is higher than that at longer wavelengths. The UL of BEDF2 is lower than that of EDF, which may be because of the doping with Bi ions reducing the excited state absorption and up-conversion of Er^{3+}. Furthermore, doping with a higher concentration of Al has better diffusivity to improve the doping

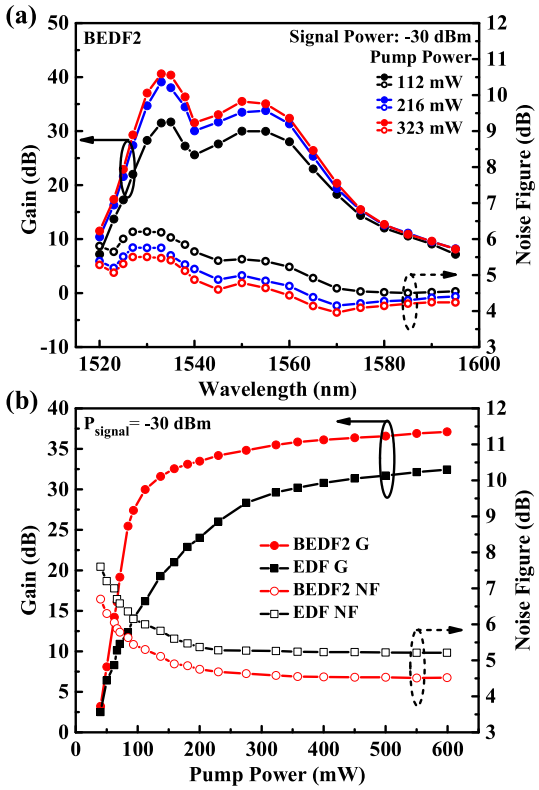

Fig. 7. Gain and NF of BEDF2 for different pump power levels with −30 dBm signal power (a). Gain and NF of EDF and BEDF2 versus pump power at 1550 nm (b).

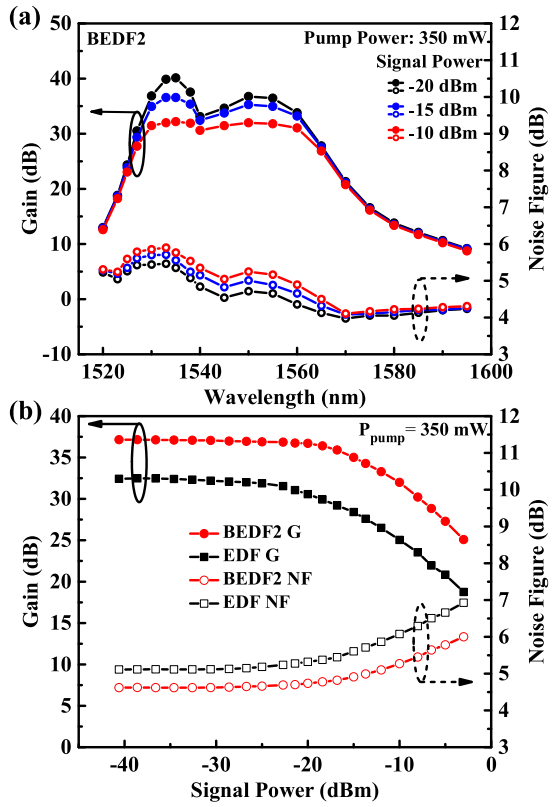

Fig. 8. Gain and NF of BEDF2 for different signal power levels with a pump power of 350 mW (a). Gain and NF of EDF and BEDF2 versus signal power levels at 1550 nm (b).

uniformity of ions and reduce the Rayleigh scattering caused by ion clusters [37], [38].

E. Amplification Characteristics

The amplification characteristics of BEDF2 and EDF were investigated. We measured the gain and NF of the forward pump for BEDF2 at different pump power levels under an input signal power of −30 dBm. The result is depicted in Fig. 7(a). With an increase in the pump power, the population inversion increases with a gradual increase in gain and saturates at a high pump power for BEDF2. NF decreases with an increase in the pump power and saturates with the gain saturation. For BEDF2, the bandwidth with a gain of more than 25 dB is approximately 42 nm (1525–1567 nm), and values of NF within the range of 1520 to 1595 nm are lower than those detected at 5.2 dB when the pump power is 323 mW. Furthermore, a minimum NF of 3.7 dB is obtained at 1570 nm, and the bandwidth with NF less than 4 dB is approximately 23 nm (1560–1583 nm) with a signal power of −30 dBm. The gain and NF of BEDF2 and EDF for different pump power levels with −30 dBm signal power at 1550 nm are shown in Fig. 7(b). With an increase in the pump power, the gain of BEDF2 increases faster than that of EDF. The gain and NF of BEDF2 and EDF at 1550 nm are 37.1 and 4.3 dB and 32.4 and 5.2 dB, respectively, at a pump power of 600 mW. These results indicate that BEDF2 has a higher gain and lower NF under the same pump power compared with those of EDF.

The amplification characteristics of BEDF2 under different signal power levels at a pump power of 350 mW are presented in Fig. 8(a). With an increase in signal power from −20 dBm to −10 dBm, the gain gradually saturates, and the maximum value of gain decreases from 40 to 32 dB at 1533 nm, while the minimum value of NF increases from 3.7 to 3.9 dB at 1570 nm. This is mainly because the intensity of the signal power increases while the population inversion relatively decreases. BEDF2 exhibits a flat gain of 30 dB with a gain ripple of less than 1.5 dB from 1527 to 1562 nm with a signal power of −10 dBm. Furthermore, NF value is high for a short span and gradually decreases when it reaches the longer wavelength span, regardless of the signal power. This is attributed to the decrease in the emission-to-absorption cross-section ratio from shorter to longer wavelength spans [2]. The gain and NF of EDF and BEDF2 at different signal power levels with a pump power of 350 mW at 1550 nm are shown in Fig. 8(b). With an increase in the signal power, the decline in the gain of BEDF2 is more gradual than that of EDF. BEDF2 exhibits lower NF and higher gain under the same signal power compared with those of EDF.

Compared to the gain and NF of EDF, BEDF2 shows a lower NF and higher gain under different conditions. According to previous studies, co-doping with Bi ions can reduce the maximum phonon energy of the fiber. A decrease in the maximum phonon energy can reduce the non-radiative transition rate, increase the number of particles at the $^4I_{13/2}$ level on Er^{3+}, thereby increasing the fluorescence lifetime of Er^{3+}. Furthermore, the longer fluorescence lifetime of BEDF2 enhances the probability of stimulated radiation and reduces the spontaneous emission probability according to the rate transfer equation for Er^{3+} ions,

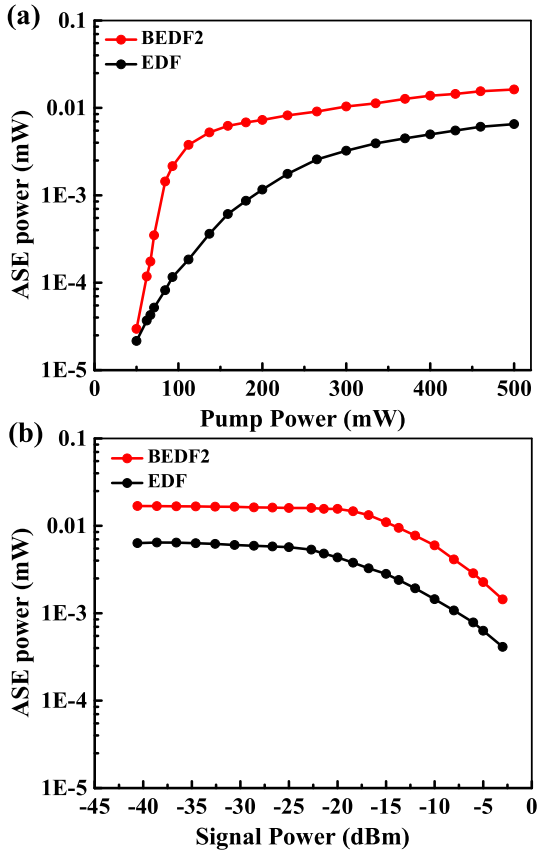

Fig. 9. The ASE power of BEDF2 and EDF with different pump power (a) and signal power (b).

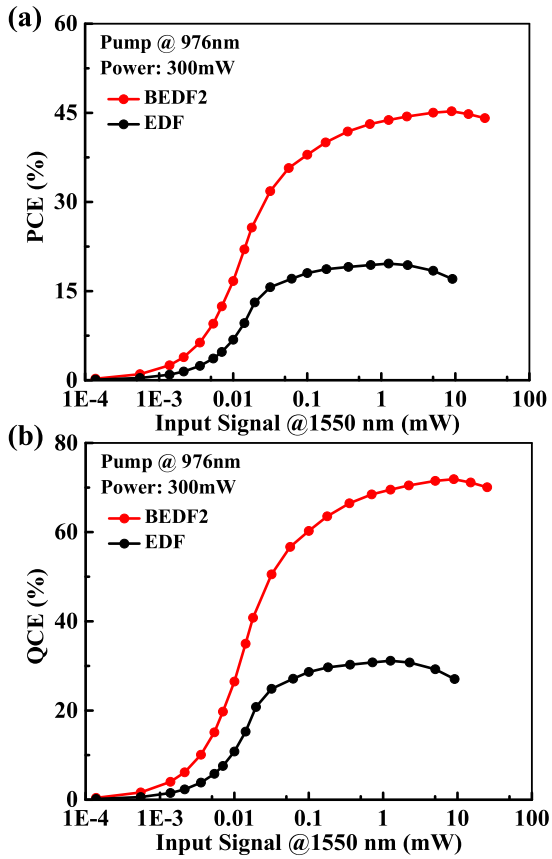

Fig. 10. Quantum conversion efficiency (a) and pump conversion efficiency (b) of BEDF2 and EDF at 1550 nm for different pump power levels at 976 nm.

leading to a further decrease in NF and an increase in gain [39]. Besides, a lower UL at the absorption wavelength improves the pump utilization. In addition, a lower UL at the emission wavelength could improve the luminous efficiency, reduce noise, and increase the gain at a lower pump power. Hence, BEDF2 has not only a higher conversion efficiency and gain but also lower NF. Moreover, the gain increases rapidly with an increase in pump power and decreases slowly with an increase in signal power, which could result in a lower NF and higher gain under a larger signal.

The ASE power is an important factor affecting NF, as shown in (1). Therefore, understanding the change in ASE power according to pump power and signal power is conducive to a more intuitive understanding of NF. During signal amplification, the stimulated absorption, stimulated emission, and spontaneous emission are in a dynamic balance. While amplifying the signal light, Er^{3+} also amplifies the spontaneous emission light, the change trend of ASE with the signal light and pump light is almost the same with the changing gain trend. Owing to the longer fluorescence lifetime of Er^{3+} in BEDF2, there are more inversion particles at the $^4I_{13/2}$ metastable level. Therefore, in addition to the higher gain of BEDF2, its ASE power is also relatively higher than that of EDF, as shown in Fig. 9. However, NF of BEDF2 is relatively lower than that of EDF because the proportion of stimulated radiation is higher than that of amplified spontaneous radiation.

F. Conversion Efficiency and Saturated Output Power

Fig. 10 shows the power conversion efficiency (PCE) and quantum conversion efficiency (QCE) of BEDF2 and EDF for a 1550 nm signal when excited at 976 nm. The maximum PCE and QCE of BEDF2 reach 45.2% and 71.8%, respectively, at 1550 nm, while those of EDF are only 19.6% and 31.1%, respectively, at a pump power of 300 mW; corresponding to input signals of 9 mW and 1 mW, respectively. BEDF2 can effectively amplify a larger signal power and higher output signal power. Note that BEDF2 has a higher QCE compared with that of EDF, mainly owing to its lower NF, higher gain, and lower UL. However, the UL at the absorption wavelength of BEDF2 remains high, which can lead to the requirement of a significantly higher pump power to achieve the desired NF and gain, making the maximum QCE slightly lower than that of 80% achieved in commercial fibers with a pump power of 100 mW [3].

The saturated output powers of BEDF2 and EDF were measured at a wavelength of 1550 nm and pump power of 350 mW as illustrated in Fig. 11. The corresponding small-signal gains of BEDF2 and EDF are 36.8 and 32.3 dB, respectively. The saturated output power of BEDF2 is 21.4 dBm at a signal input power of −12.4 dBm, corresponding to a 3 dB decrease in small-signal gain. However, the saturated output power of EDF is only 14.8 dBm when the input signal power is −14.5 dBm. A

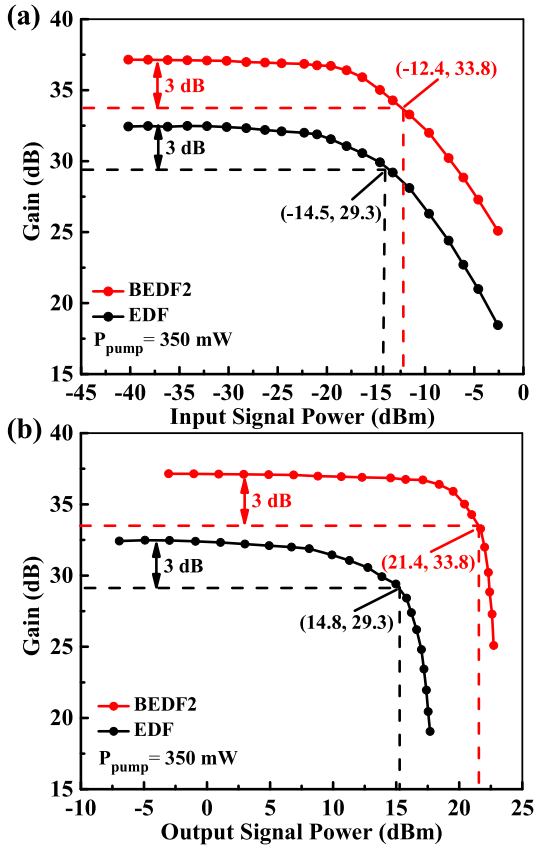

Fig. 11. Gain dependency of BEDF2 and EDF for different 1550 nm input (a) and output signal levels (b).

higher saturated output power is conducive toward amplifying a large signal.

IV. Conclusion

In this study, we investigate the spectral and amplification properties of BEDF and EDF. The Raman spectra of BEDFs and EDF showed that the maximum phonon energy of BEDF is lower than that of EDF, although the doped phosphorus concentrations in BEDF and EDF are nearly the same. This may be attributed to the co-doping of Bi, combined with the excess P in some special form, and that inhibits the formation of the P=O bonds. Because of a decrease in the maximum phonon energy of BEDF, the non-radiative transition rate can be reduced, and a possible energy transfer from BACs to Er^{3+}, which lead to a longer fluorescence lifetime in BEDF than that of EDF. The longer fluorescence lifetime of BEDF increases the population inversion level, enhances the probability of stimulated radiation, and reduces the spontaneous emission probability according to the rate transfer equation for Er^{3+} ions. And, it leads to a decrease in NF and an increase in gain. Furthermore, a lower UL at the emission wavelength of BEDF is beneficial for reducing the NF and increasing the gain. BEDF exhibits NF values lower than 5.2 dB. Moreover, its bandwidth with NF less than 4 dB is approximately 23 nm (1560–1583 nm) and with a gain of more than 25 dB is approximately 42 nm (1525–1567 nm). Meanwhile, a flat gain of 30 dB with a gain ripple of less than 1.5 dB from 1527 to 1562 nm when the signal power is −10 dBm can be observed. The maximum PCE and QCE of BEDF are 45.2% and 71.8% at 1550 nm, respectively, which are higher than those of EDF. The saturated output power is approximately 21.4 dBm at a wavelength of 1550 nm. Therefore, we conclude that this type of BEDF has considerable potential in broadband optical communication transmission.

References

[1] P. J. Winzer, D. T. Neilson, and A. R. Chraplyvy, "Fiber-optic transmission and networking: The previous 20 and the next 20 years [Invited]," *Opt. Exp.,* vol. 26, no. 18, pp. 24190–24239, 2018, doi: 10.1364/OE.26.024190.

[2] M. Pal, M. C. Paul, A. Dhar, and A. Pal, "Investigation of the optical gain and noise figure for multi-channel amplification in EDFA under optimized pump condition," *Opt. Commun.,* vol. 273, no. 2, pp. 407–412, 2007, doi: 10.1016/j.optcom.2007.01.039.

[3] L. Rapp and M. Eiselt, "Optical amplifiers for multi-band optical transmission systems," *J. Lightw. Technol.,* vol. 40, no. 6, pp. 1579–1589, Mar. 2022, doi: 10.1109/jlt.2021.3120944.

[4] D. M. Baney, P. Gallion, and R. S. Tucker, "Theory and measurement techniques for the noise figure of optical amplifiers," *Opt. Fiber Technol.,* vol. 6, no. 2, pp. 122–154, 2000, doi: 10.1006/ofte.2000.0327.

[5] A. V. Kir'yanov, V. V. Dvoyrin, V. M. Mashinsky, N. N. Il'ichev, N. S. Kozlova, and E. M. Dianov, "Influence of electron irradiation on optical properties of bismuth doped silica fibers," *Opt. Exp.,* vol. 19, no. 7, pp. 6599–6608, 2011, doi: 10.1364/OE.19.006599.

[6] I. A. Bufetov, S. V. Firstov, V. F. Khopin, O. I. Medvedkov, A. N. Guryanov, and E. M. Dianov, "Bi-doped fiber lasers and amplifiers for a spectral region of 1300–1470 nm," *Opt. Lett.,* vol. 33, no. 19, pp. 2227–2229, 2008, doi: 10.1364/OL.33.002227.

[7] E. M. Dianov, "Bismuth-doped optical fibers: A challenging active medium for near-IR lasers and optical amplifiers," *Light Sci. Appl.,* vol. 1, no. 5, 2012, Art. no. e12, doi: 10.1038/lsa.2012.12.

[8] Y. Luo, J. Wen, J. Zhang, J. Canning, and G. D. Peng, "Bismuth and erbium codoped optical fiber with ultrabroadband luminescence across O-, E-, S-, C-, and L-bands," *Opt. Lett.,* vol. 37, no. 16, pp. 3447–3449, 2012, doi: 10.1364/OL.37.003447.

[9] M. Peng, N. Zhang, L. Wondraczek, J. Qiu, Z. Yang, and Q. Zhang, "Ultrabroad NIR luminescence and energy transfer in Bi and Er/Bi co-doped germanate glasses," *Opt. Exp.,* vol. 19, no. 21, pp. 20799–20807, 2011, doi: 10.1364/OE.19.020799.

[10] Q. Zhao, J. Zhang, Y. Luo, J. Wen, and G. D. Peng, "Energy transfer enhanced near-infrared spectral performance in bismuth/erbium codoped aluminosilicate fibers for broadband application," *Opt. Exp.,* vol. 26, no. 14, pp. 17889–17898, 2018, doi: 10.1364/OE.26.017889.

[11] Q. Zhao, Y. Luo, W. Wang, J. Canning, and G. D. Peng, "Enhanced broadband near-IR luminescence and gain spectra of bismuth/erbium co-doped fiber by 830 and 980 nm dual pumping," *AIP Adv.,* vol. 7, no. 4, 2017, Art. no. 045012, doi: 10.1063/1.4981903.

[12] Z. M. Sathi, J. Zhang, Y. Luo, J. Canning, and G. D. Peng, "Spectral properties and role of aluminium-related bismuth active centre (BAC-Al) in bismuth and erbium co-doped fibres," *Opt. Mater. Exp.,* vol. 5, no. 5, pp. 1195–1209, 2015, doi: 10.1364/OME.5.001195.

[13] S. V. Firstov, K. E. Riumkin, A. M. Khegai, and S. V. Alyshev, "Wideband bismuth- and erbium-codoped optical fiber amplifier for C + L + U-telecommunication band," *Laser Phys. Lett.,* vol. 14, no. 11, 2017, Art. no. 110001, doi: 10.1088/1612-202X/aa8adf.

[14] A. A. Al-Azzawi, A. A. Almukhtar, P. H. Reddy, and S. Das, "An efficient wideband hafnia-bismuth erbium co-doped fiber amplifier with flat-gain over 80 nm wavelength span," *Opt. Fiber Technol.,* vol. 48, pp. 186–193, 2019, doi: 10.1016/j.yofte.2019.01.012.

[15] Q. Qiu, "Ultra-low noise figure in optical fiber amplifier by tailoring the mode field profile of erbium-doped fiber," *IEEE Photon. J.,* vol. 14, no. 1, Feb. 2022, Art. no. 7201106, doi: 10.1109/jphot.2021.3121728.

[16] J. Wen, J. Wang, Y. Dong, and N. Chen, "Photoluminescence properties of Bi/Al-codoped silica optical fiber based on atomic layer deposition method," *Appl. Surf. Sci.,* vol. 349, pp. 287–291, 2015, doi: 10.1016/j.apsusc.2015.04.138.

[17] J. Zheng, Y. Dong, X. Pan, and J. Wen, "Ultra-wideband and flat-gain optical properties of the PbS quantum dots-doped silica fiber," *Opt. Exp.,* vol. 27, no. 26, pp. 37900–37909, 2019, doi: 10.1364/OE.27.037900.

[18] T. Deschamps, N. Ollier, H. Vezin, and C. Gonnet, "Clusters dissolution of Yb^{3+} in codoped SiO_2-Al_2O_3-P_2O_5 glass fiber and its relevance to photodarkening," *J. Chem. Phys.,* vol. 136, no. 1, 2012, Art. no. 014503, doi: 10.1063/1.3673792.

[19] R. Deacon, R. Nicholas, and P. Shields, "Stark magnetophonon resonances in Wannier-Stark localized InAs/ GaSb superlattices," *Phys. Rev. B,* vol. 75, no. 8, 2007, Art. no. 121306, doi: 10.1103/PhysRevB.75.089903.

[20] P. B. Hansen, L. Eskildsen, J. Stentz, and T. A. Strasser, "Rayleigh scattering limitations in distributed Raman pre-amplifiers," *IEEE Photon. Technol. Lett.,* vol. 10, no. 1, pp. 159–161, Jan. 1998, doi: 10.1109/68.651148.

[21] B. Yan and Y. Luo, "Measurement of optical fibre amplifier," in *Handbook of Optical Fibers*. Berlin, Germany: Springer, 2018, pp. 1–44, doi: 10.1007/978-981-10-1477-2_45-1.

[22] B. Yan, Y. Luo, A. Zareanborji, G. Xiao, G. D. Peng, and J. Wen, "Performance comparison of bismuth/erbium co-doped optical fibre by 830 nm and 980 nm pumping," *J. Opt.,* vol. 18, no. 10, 2016, Art. no. 105705, doi: 10.1088/2040-8978/18/10/105705.

[23] Z. Zheng, "Co-doping effect of bismuth ions on the gain characteristics of Er-doped silica optical fiber," *IEEE Photon. J.,* vol. 14, no. 4, pp. 1–8, Aug. 2022, Art. no. 7146308, doi: 10.1109/JPHOT.2022.3193901.

[24] F. L. Galeener, "Planar rings in vitreous silica," *J. Non-Crystalline Solids,* vol. 49, no. 1/3, pp. 53–62, 1982, doi: 10.1016/0022-3093(82)90108-9.

[25] K. Sekimoto and T. Matsubara, "TO-LO splittings of glassy dielectrics," *Phys. Rev. B,* vol. 26, no. 6, pp. 3411–3416, 1982, doi: 10.1103/PhysRevB.26.3411.

[26] M. C. Payne and J. C. Inkson, "Longitudinal-optic-transverse-optic vibrational mode splittings in tetrahedral network glasses," *J. Non-Crystalline Solids,* vol. 68, no. 2/3, pp. 351–360, 1984, doi: 10.1016/0022-3093(84)90016-4.

[27] A. E. Geissberger and F. L. Galeener, "Raman studies of vitreous SiO_2 versus fictive temperature," *Phys. Rev. B,* vol. 28, no. 6, pp. 3266–3271, 1983, doi: 10.1103/PhysRevB.28.3266.

[28] F. Wang, C. Shao, and C. Yu, "Effect of $AlPO_4$ join concentration on optical properties and radiation hardening performance of Yb-doped Al_2O_3-P_2O_5-SiO_2 glass," *J. Appl. Phys.,* vol. 125, no. 17, 2019, Art. no. 173104, doi: 10.1063/1.5096469.

[29] C. Shao, Y. Jiao, F. Lou, and M. Wang, "Enhanced radiation resistance of ytterbium-doped silica fiber by pretreating on a fiber preform," *Opt. Mater. Exp.,* vol. 10, no. 2, pp. 408–420, 2020, doi: 10.1364/ome.384362.

[30] C. Shao, "Relationship between glass structure and spectroscopic properties in Er^{3+}/Yb^{3+}/Al^{3+}/P^{5+}-doped silica glasses," *Opt. Mater. Exp.,* vol. 10, no. 5, pp. 1169–1181, 2020, doi: 10.1364/ome.389769.

[31] B. G. Aitken, R. E. Youngman, R. R. Deshpande, and H. Eckert, "Structure−property relations in mixed-network glasses: Multinuclear solid state NMR investigations of the system xAl_2O_3:(30-x) P_2O_5:70SiO_2," *J. Phys. Chem. C,* vol. 113, no. 8, pp. 3322–3331, 2009, doi: 10.1021/jp809208m.

[32] O. V. Laguta, H. E. Hamzaoui, M. Bouazaoui, V. B. Arion, and I. M. Razdobreev, "On the nature of photoluminescence in bismuth-doped silica glass," *Sci. Rep.,* vol. 7, no. 1, 2017, Art. no. 3178, doi: 10.1038/s41598-017-03464-8.

[33] A. Pan and A. Ghosh, "Structural and optical properties of lithium bismuthate glasses," *J. Mater. Res.,* vol. 17, no. 8, pp. 1941–1944, 2002, doi: 10.1557/JMR.2002.0287.

[34] B. R. Judd, "Optical absorption intensities of rare-earth ions," *Phys. Rev.,* vol. 127, no. 3, pp. 750–761, 1962, doi: 10.1103/PhysRev.127.750.

[35] X. Zou and T. Izumitani, "Spectroscopic properties and mechanisms of excited state absorption and energy transfer upconversion for Er^{3+}-doped glasses," *J. Non-Crystalline Solids,* vol. 162, no. 1-2, pp. 68–80, 1993, doi: 10.1016/0022-3093(93)90742-g.

[36] L. Petit, T. Cardinal, and J. J. Videau, "Effect of the introduction of $Na_2B_4O_7$ on erbium luminescence in tellurite glasses," *J. Non-Crystalline Solids,* vol. 298, no. 1, pp. 76–88, 2002, doi: 10.1016/s0022-3093(01)01036-5.

[37] A. V. Kir'yanov, A. Halder, Y. O. Barmenkov, E. H. Sekiya, and K. Saito, "Discussion on Raleigh scattering as a dominant loss factor in VIS/NIR in bismuth-doped silicate fibers," *Opt. Mater. Exp.,* vol. 9, no. 7, pp. 2817–2827, 2019, doi: 10.1364/OME.9.002817.

[38] A. V. Kir'yanov, V. V. Dvoyrin, V. M. Mashinsky, Y. O. Barmenkov, and E. M. Dianov, "Nonsaturable absorption in alumino-silicate bismuth-doped fibers," *J. Appl. Phys.,* vol. 109, no. 2, pp. 1998–1986, 2011, doi: 10.1063/1.3532049.

[39] Y. Dong, Y. Zhao, and H. Zhang, "Theoretical study on ultra-broadband gain and low noise characteristics of PbS quantum dots-doped silica fiber amplifier," *Opt. Commun.,* vol. 493, 2021, Art. no. 126992, doi: 10.1016/j.optcom.2021.126992.